PERGAMON

Acta mater. 48 (2000) 2031–2047

Acta MATERIALIA

www.elsevier.com/locate/actamat

MODELING THE DEFORMATION BEHAVIOR OF HADFIELD STEEL SINGLE AND POLYCRYSTALS DUE TO TWINNING AND SLIP

I. KARAMAN[1], H. SEHITOGLU[1]†, A. J. BEAUDOIN[1], Y. I. CHUMLYAKOV[2], H. J. MAIER[3] and C. N. TOMÉ[4]

[1]University of Illinois, Department of Mechanical and Industrial Engineering, 1206 W. Green St., Urbana, IL 61801, USA, [2]Siberian Physical–Technical Institute, Revolution Sq. 1, Tomsk, 634050, Russia, [3]University of Paderborn, Lehrstuhl f. Werkstoffkunde, D-33095 Paderborn, Germany and [4]MST-8, MS G755, Los Alamos National Laboratory, Los Alamos, NM 87545, USA

(Received 18 October 1999; accepted 8 February 2000)

Abstract—Stress–strain responses of single and polycrystals of Hadfield steel were modeled using a visco-plastic self-consistent approach. A unique hardening formulation was proposed in the constitutive model incorporating length scales associated with spacing between twin lamellae and grain boundaries. TEM observations lend further support to the length scales incorporated into the constitutive model. Many of the experimental findings were made on $[\bar{1}11]$ and $[\bar{1}44]$ crystal orientations deformed in tension, displaying fine twin lamellae at small strains in addition to slip in intra-twin regions. A natural outcome of the model was the small deformation activity inside the twinned regions and higher deformations between the twins. The model utilized dislocation density as a state variable and predicted the stress–strain responses and texture evolution in single crystals accurately over a broad range of strains. The responses of polycrystals with three grain sizes (100, 300, and 1000 μm) were also captured closely with the model in addition to the twin volume fraction evolution with increasing deformation. Based on the simulations, it was possible to explain unequivocally the upward curvature in stress–strain curves in the single crystals and in coarse grained polycrystals of Hadfield steel. Overall, the combined experimental and modeling efforts provide a reliable tool to characterize slip–twin interaction in low stacking fault energy f.c.c. materials.

Keywords: Twinning; Austenite; Stress–strain relationship; Constitutive equations; Texture

1. INTRODUCTION

Hadfield steels are well known for their high strain hardening, and upward curvature in stress–strain curves [1–3]. Twinning has been observed as the main deformation mechanism [1] in these alloys. An extensive single crystal study by the authors [3] has elucidated the competing effects of slip and twinning in this material and explained the observed tension–compression asymmetry and orientation dependence of strain-hardening behavior. In the orientations which deform by twinning and slip an upward curvature of the stress–strain response was evident. In the orientations deforming only by slip, the upward curvature was replaced by a more typical f.c.c. response. The splitting of grains or single crystals into twinned and untwinned regions, and the ensuing interference of deformation by these twinned boundaries account for the "ultra" strain-hardening behavior. The present work incorporates these experimental findings in a crystal plasticity framework.

In previous crystal plasticity studies, novel constitutive frameworks were established for simulating the stress–strain response and texture evolution [4] due to slip. These modeling efforts have been largely limited to the medium and high stacking fault energy (SFE) f.c.c. materials like copper and aluminum in which twinning is insignificant at room temperature. Early studies [5–7] on twinning have focused mainly on h.c.p. materials such as Zr and Ti alloys where twinning is the main deformation mechanism. Recently, the effect of twinning on texture development and stress–strain behavior of low SFE f.c.c. metals has been a topic of intense research [6, 8, 9]. Some success was achieved in predicting the deformation of brass under plain strain compression and simple compression [6, 8]. The unique feature of twinning is that twinning-induced reorientation between the twinned region and the

† To whom all correspondence should be addressed.

1359-6454/00/$20.00
PII: S1359-6454(00)00051-3

matrix occurs in an abrupt manner. On the other hand, in slip deformation the lattice rotation is gradual. The formation of twins within the existing grains introduces additional boundaries, and this in turn governs the strain-hardening behavior and texture development. Therefore, the treatment of twinning has to include new features to the classical slip description in crystal plasticity models. Ultimately, systematic investigation of the low SFE class of materials in either single crystal or polycrystalline forms with different grain sizes will facilitate our ability to model twinning deformations, and this will be the subject of the present paper.

Previous modeling efforts in crystal plasticity either assume zero hardening [8], phenomenological power law hardening [6], or different hardening laws for each stage of deformation [9] to mimic stress–strain response. Moreover, previous treatments extract single crystal parameters from polycrystalline stress–strain response. Admittedly, grain boundaries complicate the understanding of the competing effects and interactions of twinning and slip. To advance our understanding of relative resistances of slip and twinning, the use of single crystals proves invaluable. In this study, Hadfield manganese steel single crystal experiments will be reported followed by polycrystalline stress–strain responses and texture evolution. Simulations will be presented that closely reproduce the experimental responses in all cases.

Since there is an abrupt change in orientation between a grain and the twins formed in the present material, the Taylor–Bishop–Hill or Full Constraints (FC) [10] approach and the Relaxed Constraints (RC) formulations [11] are not appropriate. In the FC formulation, the interaction of the grain or twinned regions with their surroundings is not considered. Since twins form as thin lamellae and cluster to form bundles, the interaction of twins with the surrounding matrix plays an important role in strain hardening. The RC formulation relaxes some strain components, however, its application is restricted to materials with highly distorted grains [12]. On the other hand, Lebensohn and Tomé [5] treated each grain as a viscoplastic inclusion embedded in the homogeneous medium representing the aggregate. The relation between stress and strain rate in the grain was linearized by either a tangent approach or a secant approach [5]. This formulation resulted in an interaction equation that relates the stress and strain rate in the grain with the overall stress and strain rate of the homogeneous aggregate. Both the secant and tangent approach allow for each grain to deform differently, depending on the relative directional stiffness of grain and homogeneous medium. In this study the secant approach will be modified to include strain-hardening effects associated with twinning.

The main shortcoming of crystal plasticity models incorporating twinning as a deformation mode in low SFE f.c.c. materials is the lack of a physical basis for the relation between the length scale (i.e. grain size or homogeneous deformation zone [13]) and the dislocation density evolution [14]. The hardening associated with the evolution of dislocation density is represented with a statistical storage term (athermal component) proportional to the square root of dislocation density and a dynamic recovery term proposed by Mecking and Kocks [15], leading to a well-known Voce type hardening law. Estrin and Mecking [16] remarked that the spacing between impenetrable obstacles or grain boundaries decides the mean free path (mfp) of dislocations producing a geometric contribution to the dislocation density. Their study [16] proposed that when the two storage terms (statistical and geometrical) are both used the simulations improve. This ''hybrid model'' is applicable to the materials in which the mfp is determined both by dislocation–dislocation interaction and by such barriers as grain and *twin*boundaries [16]. A recent successful application of this hybrid model by Acharya and Beaudoin [14] considered a physically motivated lattice incompatibility measure to mimic the mfp for the storage of net dislocations. In the present case, since twin formation subdivides the grains as twin boundaries act as barriers to dislocation motion, the mfp decreases with increasing volume fraction of twins assuming the mfp to be proportional to the spacing of the lamellae. Then, the strain hardening changes with the reciprocal of the mfp of dislocations. Experimental work by El-Danaf *et al.* [13] indicates an inverse dependence of the dislocation density evolution on the mfp (homogeneous deformation zone size) consistent with the model adopted in the present work.

The outline of the paper is as follows: in Section 2, the experimental details will be provided. In Section 3 the constitutive equations for single crystal and polycrystals and the viscoplastic inclusion formulation will be described. In Section 4, twinning-induced reorientation will be explained considering the predominant twin reorientation (PTR) scheme [7]. Section 5 will include a detailed explanation of the hardening approach. In Section 6 a comparison of simulations and experiments will be given.

2. EXPERIMENTAL TECHNIQUES

The material used in this study was a Hadfield manganese steel with a composition of Mn 12.34%, C 1.03%, and Fe balance. Single crystals were grown by the Bridgman technique in a He atmosphere, followed by homogenization in an inert gas at 1373 K for 24 h. Electro-discharged machining was utilized to cut the regular dog-bone shaped flat tensile specimens with nominal dimensions of $8 \times 3 \times 1\ mm^3$ in gage. Specimens were then solution treated and water quenched from 1373 K after 1 h.

Tests were performed at room temperature with a screw driven ATS test machine. For the measurement of strain, a miniature size MTS axial extensometer was employed with a 3 mm gage section. For TEM analysis, the samples were prepared by mechanical grinding and twin jet electropolishing. The electropolishing agent is a mixture of 80 g of anhydrous sodium chromate and 400 ml of glacial acetic acid. Thin foils were examined in a Hitachi H-8100 electron microscope operated at 200 kV to reveal the narrow twins and the dislocation structure. Hardness measurements were performed by a Buehler Micromet II microhardness tester. For the measurement of the texture evolution in single crystals, a Philips X'Pert MRD Goniometer was used with monochromatic Cu-K radiation. POPLA software [17] was used to extract the texture plots.

3. CONSTITUTIVE RELATIONS

Plastic deformation occurs when a slip or a twinning system becomes active. The resolved shear stress, τ^s_{RSS}, for a system (s) is given by

$$\tau^s_{\mathrm{RSS}} = m^s_i \sigma_i \tag{1}$$

where m^s_i is the vector form of the Schmid tensor and σ_i is the vector form of the applied stress. To describe the shear rate in the system s, a rate sensitive approach is utilized providing a nonlinear viscous shear rate as a power of τ^s_{RSS} in system s

$$\dot{\gamma}^s = \dot{\gamma}_0 \left(\frac{\tau^s_{\mathrm{RSS}}}{\tau^s_0} \right)^n = \dot{\gamma}_0 \left(\frac{m^s_i \sigma_i}{\tau^s_0} \right)^n \tag{2}$$

where $\dot{\gamma}_0$ is a reference rate, τ^s_0 is the threshold stress corresponding to this reference rate, and n is the inverse of the rate sensitivity index. If n is high enough, this description asymptotically approaches the rate insensitive limit [Schmid criterion in equation (1)]. The total strain rate in a crystal can be written as the sum of all potentially active systems and can be pseudolinearized as follows [5]:

$$\dot{\varepsilon}_i = \left[\dot{\gamma}_0 \sum_1^s \frac{m^s_i m^s_j}{\tau^s_0} \left(\frac{m^s_k \sigma_k}{\tau^s_0} \right)^{n-1} \right] \sigma_j = M^{c(\mathrm{sec})}_{ij}(\tilde{\sigma}) \sigma_j \tag{3}$$

where $M^{c(\mathrm{sec})}_{ij}$ is the secant viscoplastic compliance of the crystal which gives the instantaneous relation between stress and strain rate.

Following Lebensohn and Tomé [5], at the polycrystal level the same pseudolinear form can be implemented as in the case of equation (3) as follows:

$$\dot{E}_i = M^{(\mathrm{sec})}_{ij}(\tilde{\Sigma}) \Sigma_j = M^{(\mathrm{tg})}_{ij}(\tilde{\Sigma}) \Sigma_j + \dot{\Sigma}^0 \tag{4}$$

where $\dot{E}_i$ and Σ are the polycrystal strain rate and applied stress, and Hutchinson [18] demonstrates that $M^{(\mathrm{tg})} = nM^{(\mathrm{sec})}$.

Defining the deviations in strain rate and stress between the inclusion and the overall magnitudes as

$$\tilde{\dot{\varepsilon}}_k = \dot{\varepsilon}_k - \dot{E}_k \tag{5}$$

$$\tilde{\sigma}_j = \sigma_j - \Sigma_j \tag{6}$$

and utilizing Eshelby's inhomogeneous inclusion formulation one can solve the stress equilibrium equation to derive the following interaction equation [19]:

$$\tilde{\dot{\varepsilon}} = -\tilde{M} : \tilde{\sigma} \tag{7}$$

The interaction tensor $\tilde{M}$ is defined as

$$\tilde{M} = n(I - S)^{-1} : S : M^{(\mathrm{sec})} \tag{8a}$$

where $M^{(\mathrm{sec})}$ is the secant compliance tensor for the polycrystal aggregate and S is the viscoplastic Eshelby tensor [19].

Two remarks concerning the viscoplastic self-consistent formulation are due at this point. First, the Eshelby tensor is a function of the compliance $\mathrm{M}^{(\mathrm{sec})}$ and the ellipsoidal inclusion axes, and can be calculated considering a small compressibility and using the approximate penalty method [19]. Or else, it can be calculated exactly for an incompressible medium [20]. In either case, it should not be confused with the classical elastic Eshelby tensor.

Secondly, the interaction tensor $\tilde{M}$ in equation (8a) corresponds to a tangent formulation, and follows from using the relation $M^{(\mathrm{tg})} = nM^{(\mathrm{sec})}$ and assuming that the tangent form of equation (4) is valid locally in the homogeneous effective medium (HEM). If, instead, one assumes that the secant form of equation (4) is locally valid, then an interaction tensor of the form

$$\tilde{M} = (I - S)^{-1} : S : M^{(\mathrm{sec})} \tag{8b}$$

results. The difference between the tangent and the secant formulation is that the latter is characterized by a more rigid interaction between grain and matrix, and allows for smaller strain deviations from the average.

In this work we assume a secant type formulation. The results of the tangent formulation are qualitatively similar. Equations (3)–(8a) provide the required relations to derive $\dot{\varepsilon}$ and σ for each crystal.

The macroscopic secant compliance, $\mathrm{M}^{(\mathrm{sec})}$, can be determined by substituting equations (3) and (4) in equation (7). The macroscopic strain rate was evaluated by taking the weighted average of crystal strain rates over all the crystals as follows:

$$M^{(\mathrm{sec})} = \langle M^{c(\mathrm{sec})} : (M^{c(\mathrm{sec})} + \tilde{M})^{-1} : (M^{(\mathrm{sec})} + \tilde{M}) \rangle \tag{9}$$

Iterative solution of equations (3), (7) and (9) gives the stress in each crystal, the crystal's compliance tensor, and the polycrystal compliance consistent with the applied strain rate $\dot{E}$. In this work, n [in equation (2)] was chosen to be in the rate insensitive limit ($n = 20$). As for the interaction equation (8a),

an effective value of $n = 1$ is used corresponding to a rigid interaction.

4. TWINNING REORIENTATION SCHEME

The main issue in the incorporation of twinning into constitutive models is associated with the reorientation of a grain upon twinning. Since twinned and untwinned regions have different orientations, tracking a large number of orientations during the deformation increases computation times. In the present study, the predominant twin reorientation (PTR) scheme is utilized to tackle this problem. In this scheme, the real volume fraction of twinning in the polycrystal aggregate is defined as [7]

$$f_{\mathrm{R}} = \sum_{r} f^{r} \sum_{t_i} (g^{r,t_i}/s^{t_i}) \tag{10}$$

where g^{r,t_i} is the accumulated twinning shear associated with each twinning system t_i over the deformation steps in each crystal, s^{t_i} is the characteristic shear of the twin system and f^r is the weight of the crystal which corresponds to the volume fraction of the crystal in the aggregate. Whenever a whole crystal is reoriented by twinning, the effective twin volume fraction is updated as

$$f_{\mathrm{E}} = \sum_{r} f^{r} \Delta^{r} \quad \Delta^{r} = 0 \text{ when the crystal is untwinned} \quad \Delta^{r} = 1 \text{ when the crystal is twinned} \tag{11}$$

where r represents the number of crystals in the aggregate. At every deformation step, the fraction accumulated in the individual twinning systems of each grain $g^{r,t_i}/s^{t_i}$ is compared with a threshold value f_{T} that follows the empirical relation

$$f_{\mathrm{T}} = A_1 + A_2 \frac{f_{\mathrm{E}}}{f_{\mathrm{R}}} \tag{12}$$

where A_1 and A_2 can be determined from single crystal experimental results. The characteristics of this scheme are that it favors the reorientation of crystals using the most active twinning systems. In addition, the self-adjusting nature of the scheme guarantees the reoriented volume fraction, f_{E}, to coincide with the real volume fraction, f_{R}. Whenever f_{E} is larger than f_{R}, the threshold f_{T} increases and inhibits further reorientation by twinning until the real volume fraction catches up with the effective one. The value of the constants A_1 and A_2 was taken by Tomé *et al.* [7] as 0.25 to model large strain deformation, meaning that whenever a crystal's twin fraction reaches 50% it is reoriented using the most active twinning orientation. However, since the unique feature of Hadfield steel is the early formation of twinning (< 5% strain), these constants are chosen here as 0.15 to provide activity at small strains. Later, the self-adjusting character of the scheme accounts for the initial increase in the effective twin volume fraction.

In the present material, this approach provides an excellent agreement with experimental observations because in polycrystals one twinning system prevails at moderate strains in each crystal. For this scheme to be statistically meaningful, many grains with the same initial orientations were assumed based on their initial weight. This allowed grains with similar orientations but with different neighborhoods to favor different systems and predict texture evolution accurately. Moreover, in the single crystal case, a total number of 1000 grains was used with initially the same crystallographic orientation.

In the light of recent experimental observations [3], a new hybrid hardening relation was introduced and incorporated in the viscoplastic self consistent (VPSC) model in the following section. This treatment predicts the stress–strain behavior of Hadfield steel single and polycrystals considering both the dislocation density and volume fraction of twins as microstructural variables.

5. THE STRAIN-HARDENING FORMULATION

In continuum crystal plasticity theories, permanent deformation is accounted for by allowing slip to lead to an incompatible plastic deformation at the local level [14]. Since the total deformation is compatible, a lattice or elastic deformation accounts for the difference between the total compatible and local incompatible plastic deformation. Twinning produces similar incompatibilities in plastic deformation. This incompatibility arises from the boundary misorientation and incoherency of the twin and the matrix, and the necessity of dislocations at twin–matrix interface to accommodate the incoherency as noted by Remy [21]. It is a well-known fact that twin boundaries are a particular case of grain boundary with a low index of coincidence $\Sigma = 3$ [21]. The idea of whether twin boundaries can play a similar role as grain boundaries in low SFE f.c.c. materials in terms of blocking the dislocation motion has been proposed by Remy [21] and his approach has been supported by TEM observations [21, 22]. The twinning reaction at the twin–matrix boundary for a Co–Ni alloy was observed to be [21]

$$\frac{1}{2}[110] \rightarrow \frac{1}{2}[101]_{\mathrm{T}} + \frac{1}{6}[2\bar{1}\bar{1}]$$

slip in the matrix = slip in the twin + glissile partial in the boundary. (13)

Although this reaction is energetically unfavor-

able, under the application of stress, unfavorable dissociations become possible because they produce shear compatibility or stress relaxation. However, observation of partial dislocations in the boundary indicates that product dislocations in the boundary are not completely glissile. An important feature in the present material and in most of the low SFE f.c.c. materials with high concentration of solute atoms is that twins cluster to form bundles a few tenths to a few micrometers thick with thin layers of matrix between them. This is clearly shown in the TEM image for Hadfield steel (Fig. 1). Interestingly, it is noted that these twins do not grow to form thicker twins and they are stable after unloading. Venables [23] and Friedel [24] proposed the following reactions preceding reaction (13) to rationalize these observations

$$\frac{1}{2}[011] + \frac{1}{6}[2\bar{1}\bar{1}] \rightarrow \frac{1}{3}[111]$$

slip in the matrix + glissile partial in the boundary

= sessile Frank partial in the twin (14)

$$\frac{1}{3}[111] \rightarrow \frac{1}{6}[112] + \frac{1}{6}[110]$$

sessile Frank partial in the twin

= Shockley partial in the matrix

+ stair-rod at the boundary. (15)

From these reactions it is expected that twin boundaries can be treated as grain boundaries, especially with increasing strain and increasing sessile stair-rods or Frank partials. The dislocations in the matrix form pile-ups near a twinning boundary and lead to stress concentration near the boundary. The TEM image in Fig. 2 indicates the different slip activities in the matrix and in the twin. Since twinning forms at the early stages of deformation in this material and due to the sessile dislocation formations, most of the slip activity and thus accommodation of plastic deformation by slip occurs in the matrix. Therefore, it is believed that this constraint for deformation due to twin boundaries and twin–slip interaction provides the high strain hardening in this material. In one respect, twin boundaries can be thought of either as impenetrable obstacles or as boundaries inducing formation of finer grain sizes by subdivision of grains. This reasoning supports the choice of Estrin and Mecking's [16] hybrid hardening approach in the VPSC formulation.

In the classical Mecking and Kocks [15] plasticity

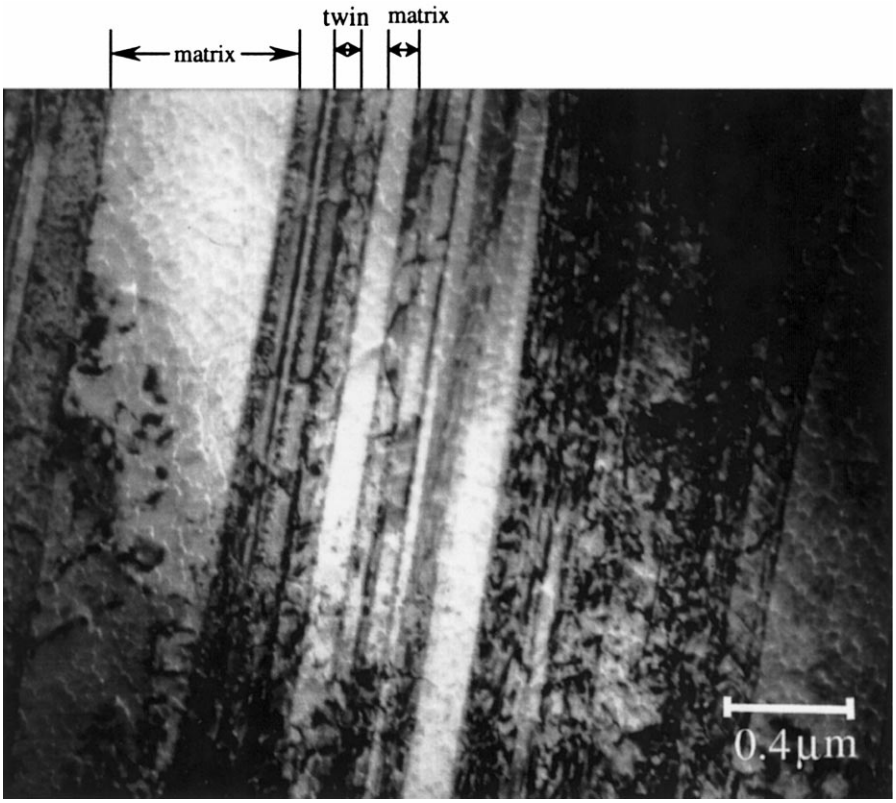

Fig. 1. TEM micrograph of the [$\bar{1}$11] oriented single crystal specimen deformed under tension at room temperature. Strain, 3%. Individual thin twins cluster to form bundles with thin layer of matrix between adjacent microtwins.

model, the kinetic of plastic deformation is determined by a single structure parameter. This parameter is the average dislocation density ρ [14]. In this phenomenological model, the evolution of the dislocation density is governed by athermal hardening and dynamic recovery components [14–16]. The athermal hardening component is represented by dislocation storage from geometrical or statistical considerations. Statistical dislocation storage originates from dislocations becoming immobilized by forest dislocations upon travelling a distance (mfp) proportional to $\rho^{1/2}$. Based on TEM observations, twin boundaries and grain boundaries both act as obstacles to dislocation motion. Thus, the increase in twin volume fraction leads to a decrease in the mfp of dislocations. To account for this effect, we consider an evolution equation for the dislocation density in the form

$$\dot{\rho} = \sum_k \left\{ \frac{K_0}{db} + k_1\sqrt{\rho} - k_2\rho \right\} |\dot{\gamma}^k| \qquad (16)$$

where d is the distance between twins or the grain size in the case of polycrystals, b is the Burgers vector, k_1 and k_2 are constants and K_0 is a geometric constant. The first term represents an empirical geometric storage term due to twin boundaries as being a barrier to dislocation motion and the second term represents the athermal (statistical) storage of moving dislocations. The third term is associated with the dynamic recovery. The d^{-1} dependence of the evolution of dislocation density (first term) coincides with the Estrin and Mecking [16] treatment. This hybrid model applies to processes in which the dislocation mfp is determined both by dislocation–dislocation interactions and by such barriers or sinks as grain and twin boundaries. In the case of twins evolving in the form of very thin lamellae (as in the case of low SFE steels), many additional twin boundaries are introduced that act as barriers to dislocation motion and, therefore, a fine grained material is mimicked. The spacing between twins is almost constant as it can be seen in the TEM image (Fig. 3) and thus, the rate of evolution of dislocation density is inversely proportional to the distance between twins. Although twins can be penetrable, a perfect dislocation splits into partials producing storage of the partials at the boundary [reactions (13)–(15)]. The formation of such pile-ups at the boundary provides the necessary ground for considering twin boundaries as barriers to dislocation motion.

The flow stress at a finite temperature and strain rate is defined following Kocks *et al.* [25], Kocks [26] and Mecking and Kocks [15] together with the Bailey–Hirsch relationship as

$$\hat{\tau} - \hat{\tau}_0 = \alpha\mu b\sqrt{\rho} + \hat{\tau}_i \qquad (17)$$

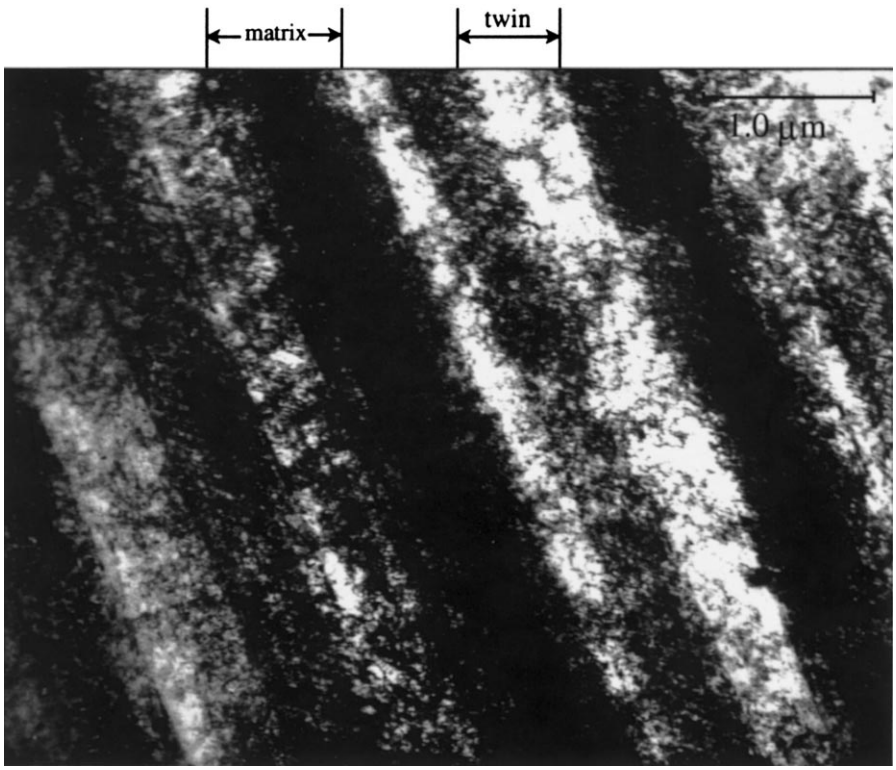

Fig. 2. TEM micrograph of the [$\bar{1}$11] oriented single crystal specimen deformed under tension at room temperature. Strain, 35%. Dislocation activity is more significant in the matrix than in the twinned regions.

where $\hat{\tau}_0$ is the yield strength, α is a constant, μ is the shear modulus, and $\hat{\tau}_i$ is the contribution of solid solution hardening. Since the nature of the interaction of the first and second term has not been completely understood up to date, a simple superposition is utilized following Kocks *et al.* [25]. It should be noted that in a more general treatment, $\hat{\tau}_i$ and equation (17) should be modified to account for kinetics of flow. However, single temperature and strain rate experiments are addressed herein.

Upon combining equations (16) and (17) and with the distance d between neighboring twins evaluated directly from Fullman's volumetric analysis [27]

$$\frac{1}{d} = \frac{1}{2t}\frac{f}{1-f} \tag{18}$$

where t is the thickness of twins and f is the volume fraction of twinned regions. Differentiating with respect to time we obtain the following expression for single crystal hardening:

$$\dot{\hat{\tau}} = \left[\frac{K_0\alpha^2\mu^2 b}{4(\hat{\tau}-\hat{\tau}_0)}\frac{1}{t}\frac{f}{1-f} + \left\{\frac{\alpha\mu b}{2}k_1 - k_2\frac{\hat{\tau}-\hat{\tau}_0}{2}\right\}\right] \sum_k |\dot{\gamma}^k| + \dot{\hat{\tau}}_i. \tag{19}$$

The thickness, t, of the twins in Hadfield steel stays almost constant after they reach a limiting value of $\sim$100–200 nm as seen in Fig. 3.

The curly bracket term in equation (19) is the well-known Voce-form hardening, which can be rewritten as [19]

$$\dot{\hat{\tau}} = \left[\frac{K_0\alpha^2\mu^2 b}{4(\hat{\tau}-\hat{\tau}_0)}\frac{1}{t}\frac{f}{1-f} + \theta_0\left\{\frac{\hat{\tau}_s-\hat{\tau}}{\hat{\tau}_s-\hat{\tau}_0}\right\}\right] \sum_k |\dot{\gamma}^k| + \dot{\hat{\tau}}_i \tag{20}$$

where θ_0 is the constant strain-hardening rate and $\hat{\tau}_s$ is the saturation stress in the absence of geometric effects.

In the case of polycrystals, when both grain and twin boundaries are present, a decision has to be made on the relative strength of these boundaries. Dislocations can dissociate [21] at twin boundaries, and the products of these dissociations can penetrate into the twinned region readily. In the case of grain boundaries, considerable pile up of dislocations is needed before slip in successive grains can be activated. Therefore, grain boundaries constitute stronger barriers and should be considered separately in the hardening formulation. Consequently, equation (20) is modified as follows:

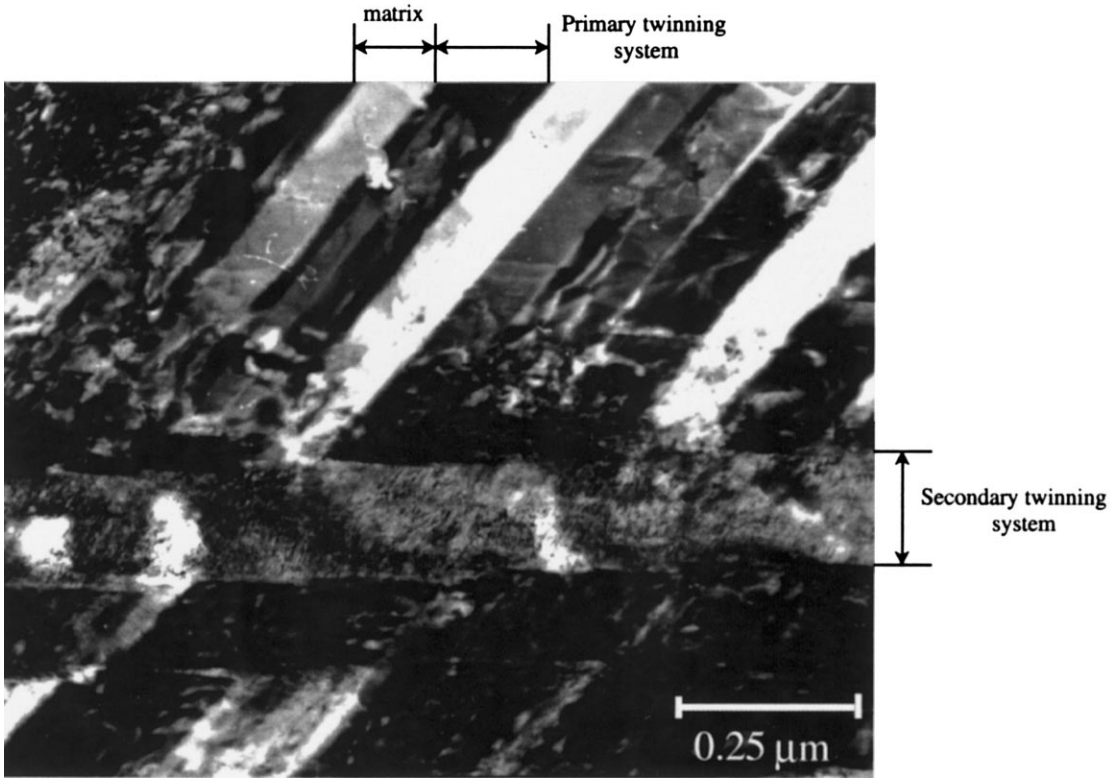

Fig. 3. TEM micrograph of the [$\bar{1}$11] oriented single crystal specimen deformed under tension at room temperature. Strain, 35%. Two twinning systems are active. Matrix–twin lamellae are obvious.

$$\dot{\hat{\tau}} = \left[\frac{\alpha^2 \mu^2 b}{2(\hat{\tau} - \hat{\tau}_0)} \left(\frac{K_0'}{d_1} + \frac{K_0''}{d_2} \right) + \theta_0 \left\{ \frac{\hat{\tau}_s - \hat{\tau}}{\hat{\tau}_s - \hat{\tau}_0} \right\} + \frac{\partial \hat{\tau}_i}{\partial \gamma} \right] \sum_k |\dot{\gamma}^k| \quad (21)$$

where d_1 [equation (18)] and d_2 are the distances between twin boundaries and grain boundaries, respectively. The different values of K_0 are utilized to represent the different strengths of boundaries.

It is also possible to treat both types of boundaries with the same strength and assign polycrystals with different grain sizes a different amount of initial twinning volume fraction. However, simulations indicated that equation (21) provides a better prediction of stress–strain response compared with the "equal" boundary strength approach.

In the present material, dynamic recovery is not a significant softening mechanism as in the case of the high SFE metals. Moreover, the statistical dislocation storage occurs by means of solid solutions more than one due to forest dislocations at low and moderate strains. Therefore, the Voce term in equation (21) is not significant in the present material. However, this term may have a significant contribution to strain hardening in the other low SFE materials such as Cu and Ag alloys. This is because of the fact that in those materials, since matrix strength is quite low, twinning is usually observed in late stage II or in stage III as a competing mechanism to cross-slip [23, 28]. Therefore, cross-slip and climb of dislocations can be the case together with twinning as a softening mechanism and the Voce term should be considered in those materials. However, in the present case, the matrix strength is high due to interstitial solid solution hardening. The primary source of strain hardening follows from slip–twin interaction and therefore, the dynamic recovery does not play a significant role on the stress–strain behavior at low and moderate strains. Thus, it will not be considered further in this study, and $\theta_0 = 0$.

The solid solution hardening contribution, $\hat{\tau}_i$, to flow stress should include the volume fraction of solid solution, the type of solution (interstitial or substitutional), and the misfit parameters (size or modulus). However, in the presence of the slip–twin interaction, solid solution hardening plays a secondary role similar to grain boundary strengthening. Therefore, the last term in equation (21) is only significant for the stage I of the present stress–strain behavior in the single crystals. Since the stage I strain-hardening coefficient is constant and independent of strain [29] in pure metals, $\partial \hat{\tau}_i / \partial \gamma$ is assumed to be constant as a first approximation in this study to predict the easy glide regime. However, the authors are currently investigating the nature of the effect of the interstitial atoms on the stage I hardening of low SFE steels and it will be reported in the near future.

As a result, the first term in equation (21) arising from slip–twin interaction by means of determining mfp of dislocations by twin or grain boundaries describes the experimental stress–strain behavior in the Hadfield steel single and polycrystals.

6. RESULTS

6.1. Single crystals

The single crystal orientation $[\bar{1}11]$ was chosen for testing the constitutive model proposed. Stress–strain and texture evolution simulations were made utilizing the twinning reorientation and strain-hardening schemes described in Sections 4 and 5. Since the VPSC model is a polycrystal plasticity model, an initial single crystal was treated as a polycrystal aggregate by splitting it into a total of 1000 grains with the same initial orientation. Throughout the present study, grains are assumed to be equiaxed in both single crystals and polycrystals. Since simulations are conducted until moderate strains, no shape update of the grains is considered. The initial critical resolved shear stresses for both slip and twinning is obtained from experimental results such that slip and twinning resistances are similar, with a slightly lower slip resistance. Consistent with our knowledge, twinning is observed at the early stages of deformation but slip is first required to nucleate twinning [3]. The rate sensitivity was selected to be represented by $n = 20$.

Since twinning develops at the early stages in this material, the twinning reorientation scheme was activated at 4% strain consistent with experimental observations [3]. As a consequence, the constants A_1 and A_2 in equation (12) were set to 0.15 to reproduce this behavior in the $[\bar{1}11]$ orientation under tension. For the aforementioned strain-hardening approach, the value for $\partial \hat{\tau}_i / \partial \gamma$ in equation (21) is derived from the experimental stress–strain response of the $[\bar{1}11]$ orientation. Since initial hardening rate is small due to a Lüders type propagation, it is taken as $\mu/4000$ for both slip and twinning. The initial value of the mechanical threshold was set to $\tau_0 = 110$ MPa for slip and $\tau_0 = 115$ MPa for twinning considering the requirement of coplanar slip before twinning. Twins are very narrow and remain at constant width of 100–200 nm during deformation. Therefore, for the hardening part in equation (21) originating from the geometrical dislocation storage, the thickness t was set to 100 nm, the value of α was 1/3 [30], K_0' was 0.1 and K_0'' was zero for the single crystal case.

The axial stress–axial strain response of the $[\bar{1}11]$ orientation under tension is shown in Fig. 4 together with the VPSC predictions. A correct trend with an upward stress–strain response was

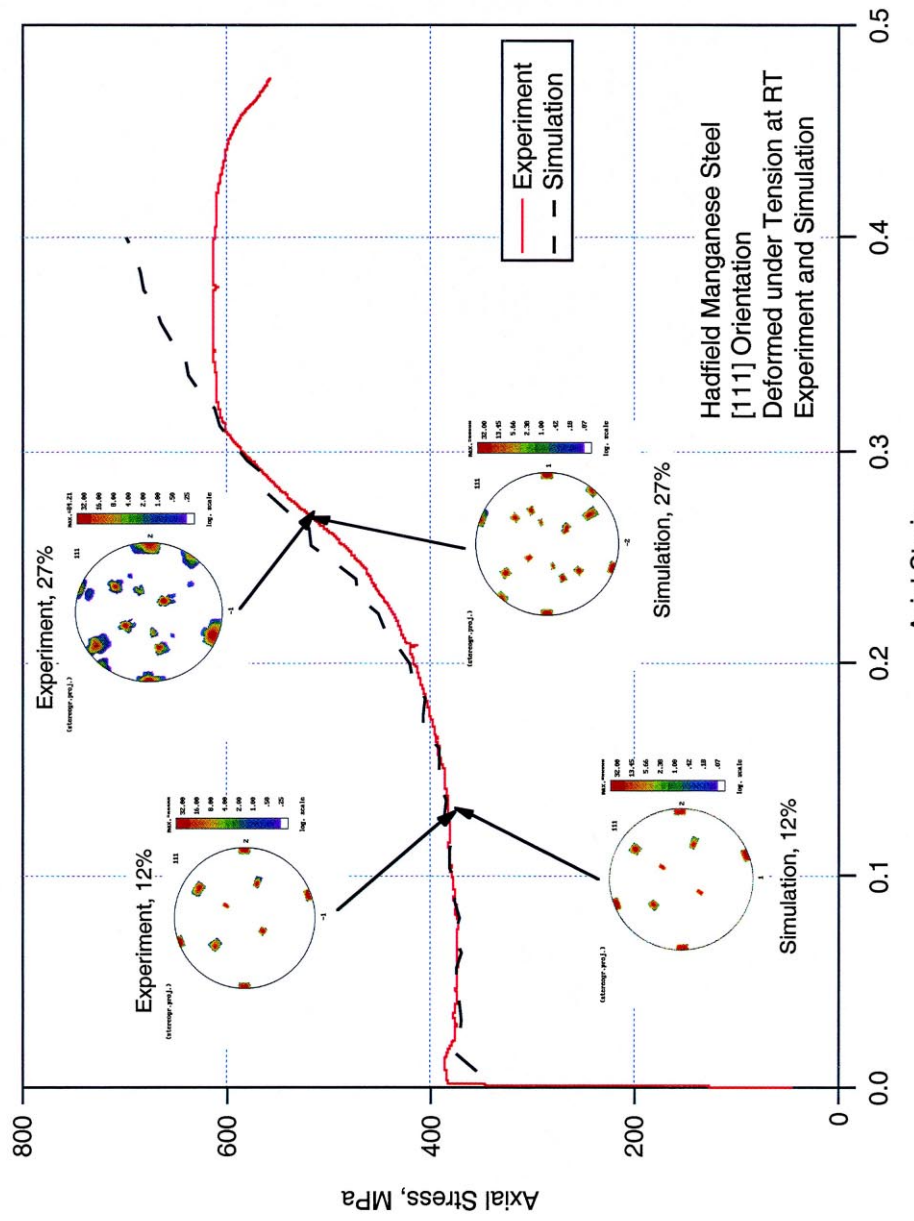

Fig. 4. The stress–strain response of the $[\bar{1}11]$ orientation deformed under tension at room temperature. Experiment and simulation. Experimental texture evolution is also shown together with simulations. The same number of twinning systems are predicted as observed in the experiments.

captured in the simulations utilizing the above parameters. The evolution of texture with increasing strain is also included in this figure. Both experimental texture measurements and simulations are incorporated in Fig. 4. In the easy glide region (at 12% strain), only one twinning system was active as noted in the [111] pole figure. Once the primary twinning system occupies the entire gage section and the secondary twinning system is activated, an increase in strain hardening is observed. From the micrograph shown in Fig. 3, it appears that only two twinning systems are active in this high strain-hardening regime. Note, however, that the area shown is quite small, and not all twins are always in contrast. Texture measurements have indeed proved that three systems were in effect as shown by the [111] pole figure at 27% strain in Fig. 4. The model was able to predict the correct number of systems at 12 and 27% strains in Fig. 4. The model also indicates that the only plane in which twinning is not activated is the one parallel to the applied load direction.

Since the [$\bar{1}$11] orientation is a symmetric orientation, the rotations due to slip are not as significant as twin rotations at low strains. Therefore, it is difficult to ascertain the slip activity from the experimental pole figures in Fig. 4. To illustrate the results further, Fig. 5 demonstrates the relative slip and twin activities in this orientation obtained from the simulations. Relative activity is defined as

$$RA_{\text{mode}} = \frac{\sum_n f^n \sum_{s'(\text{mode})} \Delta\gamma^{n,s'}}{\sum_n f^n \sum_{s(\text{all modes})} \Delta\gamma^{n,s}} \tag{22}$$

where the numerator indicates total plastic shear contribution from a single mode (slip or twinning) and the denominator is the total plastic shear (including both slip and twinning) weighted by the grains' volume fractions. Since the Schmid factor for twinning is greater than that for slip in this orientation and the CRSSs for the slip and twinning are approximately the same, the initial "twin activity" is significantly higher than the slip activity. In the easy glide regime, the twin and slip activities remain constant due to the Lüders type propagation. At higher strains, the slip activity surpasses the twin activity. Figure 5 also includes the volume fraction evolution of the twinned regions. The twin volume fraction saturates at high strains consistent with the decrease in twinning activity. At large strains, the plastic deformation is accommodated predominantly by slip.

Once twins have formed, deformation inside a twin becomes less likely, as observed experimentally (Fig. 2). The reason for this observation may be twofold. One possibility is the hardening of the twinned regions relative to the matrix lowering their deformation rate due to twin reorientation with respect to the applied stress direction. Another reason is a change in the mobility of existing dislo-

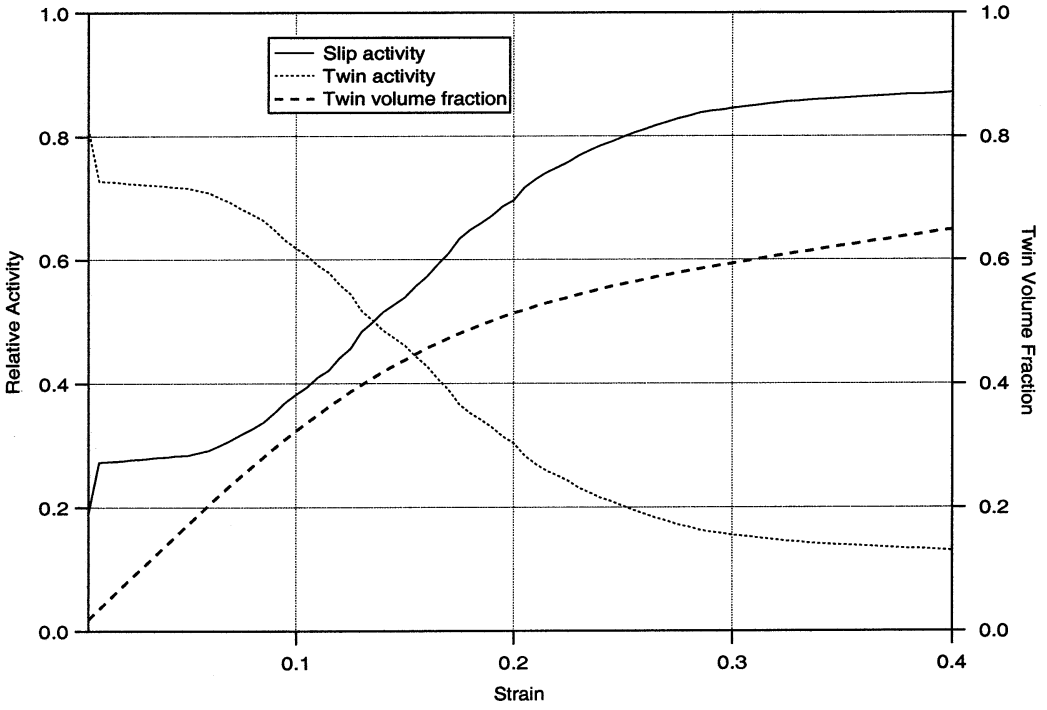

Fig. 5. The relative slip and twinning activity in the [$\bar{1}$11] crystal deformed under tensile loading at room temperature and the twin volume fraction evolution with strain obtained by the present model.

cations in the twinned regions [31]. Embury and coworkers [31, 32] propose dislocations within twins have a sessile configuration and serve as forest dislocations. This would enhance the higher hardening rate in the twinned regions. To check this theory, the relative hardness of a twin and the matrix was measured with a microindenter at 15% strain. The hardness increase in the twin was observed to be around 20% relative to the matrix at the same strain level. To determine whether an orientation change or configuration change of dislocations is responsible for the hardness increase, other measurements have been conducted at 35% strain showing approximately 35–40% increase in the twin hardness. These findings support the idea that there is an effect of the configuration change of the dislocations by twinning.

Thus, the model was modified such that once a region twins, the slip and twin resistances (CRSSs) were increased 20% in the twinned regions. In Fig. 6, the relative activities for twinned and untwinned regions are compared. As noted in Fig. 6 the twinning activity within the twins decreases rapidly. While slip accommodates the deformation inside the twins, it is not as significant as the slip or twinning activity in the matrix. Figure 6 indicates that the average number of activated systems is three to four inside the twins and these are predominantly slip systems.

In the [$\bar{1}$11] orientation, the final low hardening region cannot be predicted with our model. As discussed in an earlier study [3], it is believed that the formation of cracks at the twin–twin intersection instigates softening and failure as proposed by Mullner [33]. Therefore, this is not a model deficiency, and indeed experiments in compression confirm that the upward curvature behavior extends to high strains compared with the tension case. To check the validity of our model parameters critically, a second orientation, [$\bar{1}$44], was studied under tension. This orientation also deforms by combined twinning and slip. However, it does not exhibit the softening region before failure as can be seen in Fig. 7. Simulations in this case reproduce correctly the upward curvature of the stress–strain response seen in the experiments. This suggests that the model parameters hold in general and should be applicable to polycrystal aggregates. To test the model for polycrystal applications, additional simulations were conducted as described below.

6.2. *Polycrystals*

Simulations were performed without altering the material parameters established from the [$\bar{1}$11] case. Three different grain sizes (100, 300, and 1000 μm) are studied to investigate grain size and initial texture effects on the strain hardening. Initial textures for these three cases were measured experimentally and utilized in the model. Especially in the coarse

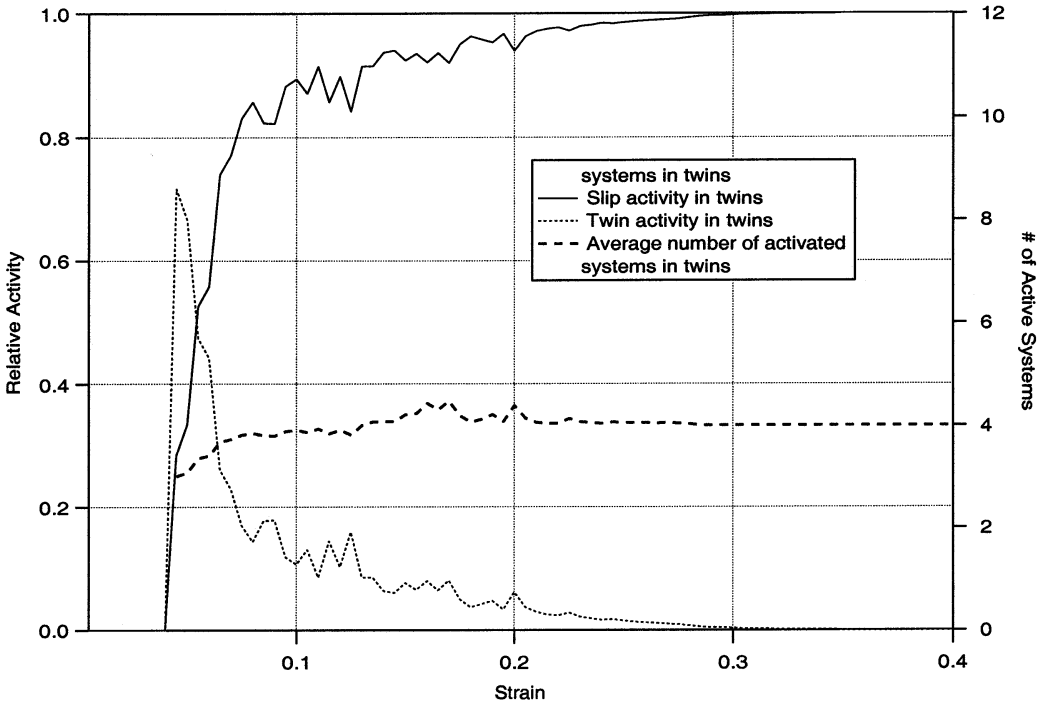

Fig. 6. The relative slip and twinning activity inside the twinned regions in the [$\bar{1}$11] crystal deformed under tensile loading at room temperature. The total number of active systems are also included in the figure. The active systems are mostly slip systems.

grain size (300 and 1000 μm) cases, an initial texture was observed, however, in fine grain size material, texture was nearly random. In initially textured cases, grains were favorably oriented for twinning (near the [$\bar{1}$11] pole). The original volume fraction associated with each grain is split into several "sub-grains" with the same orientation to be statistically meaningful in terms of our twinning reorientation scheme as explained in Section 4. A grain having 1% volume fraction of the sample is split into four sub-grains. The number of grains in the model was chosen to be approximately 2000 for the coarse grain cases and 3000 for the fine grain case. Each grain was assigned a weight (volume fraction) depending on the initial experimental texture measurements. To account for the presence of grain boundaries, they were treated separately from twin boundaries as discussed in Section 5. Equation (21) was utilized with K_0'' chosen to be 0.8 for the grain boundaries and K_0' was maintained at 0.1 for the twin boundaries.

The experimental stress–strain responses for the three different grain sizes are shown in Fig. 8 together with model predictions. An excellent agreement was observed between the experiments and the simulations. The coarse grain size cases (300 and 1000 μm) exhibited an upward curvature in the stress–strain response similar to the single crystal case, however, in the fine grain size case, the upward curvature is not apparent. The random texture in the fine grain case is conducive to strong slip activity that does not produce an upward curvature [3] in the stress–strain response. As a consequence, the randomly oriented grain aggregates exhibit an effective linear hardening that is predicted well with the model.

Figures 9 and 10 indicate the relative activities of slip and twin modes for grain sizes 300 and 100 μm, respectively. The effect of initial grain size and initial texture can be observed in these activities. The twin activity is higher than the slip activity in the coarse grain size in the early stages of the deformation. In the fine grain size case slip activity dominates. Both predictions are consistent with the general experimental observation that twinning is suppressed in fine grained materials. The coarse grain size cases have an initial texture that favors twinning. At the later stages of straining, twinning activity decreases significantly in the case of the coarse grain size because of the fast increase in the twin volume fraction. A saturation in twin volume fraction occurs at high strains but this saturation volume fraction is smaller in the fine grain size case.

Figures 9 and 10 also include the twinning and slip activity inside the twin regions. Similar to the single crystal results, plastic deformation within the twins is mostly accommodated by slip in the coarse grain size case. In the fine grain size case, the twinning and slip activities are almost equal. The higher twin volume fraction in the coarse grain size case inhibits further twin nucleation inside the twins. Similar but less potent constraint is operative for

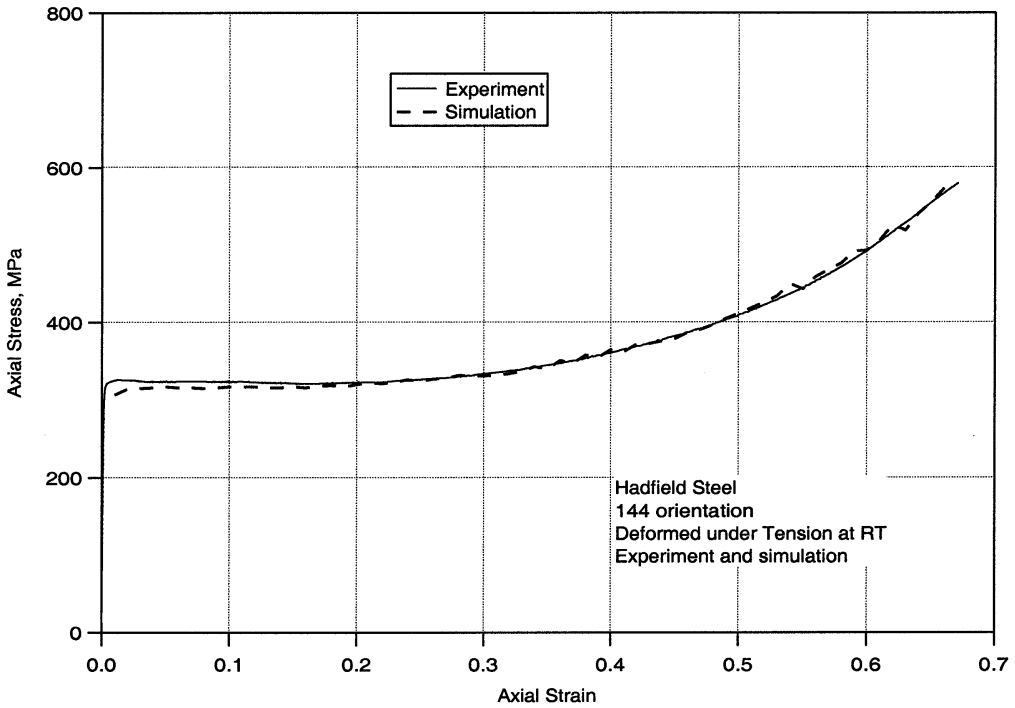

Fig. 7. The stress–strain response of the [$\bar{1}$44] orientation deformed under tension at room temperature. Experiment and simulation.

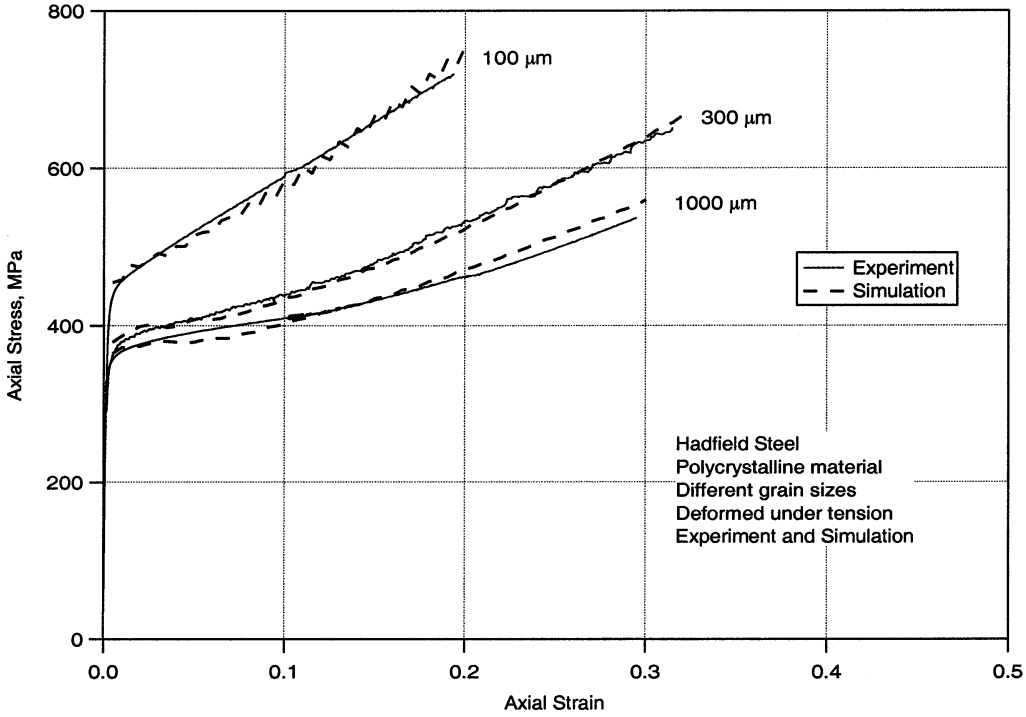

Fig. 8. The stress–strain responses of polycrystalline Hadfield steel with three different grain sizes (100, 300, and 1000 μm).

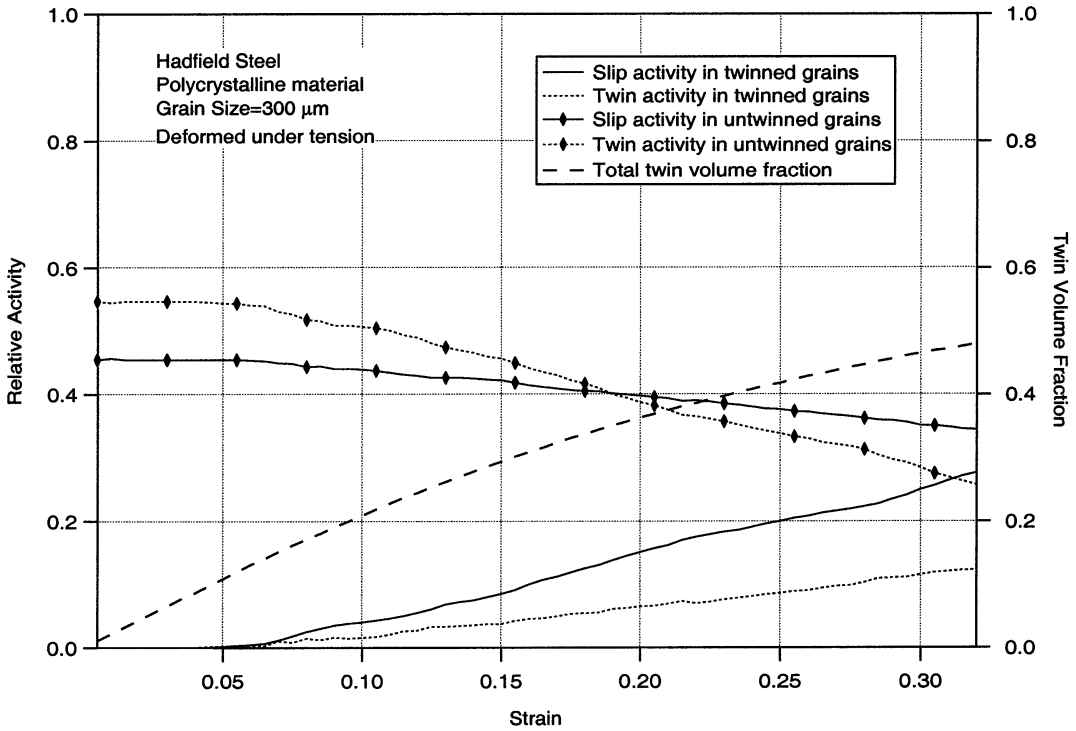

Fig. 9. The relative slip and twinning activity inside the twinned regions in the polycrystals with a grain size of 300 μm. The simulation of the twin volume fraction evolution is also included in the figure.

the fine grain size with low total twin volume fraction. One possible reason for this activity difference of slip and twinning inside the twins can be the relative orientations of twinned grains due to initial texture differences. Once a grain initially oriented favorably for twinning twins, then the applied stress direction can favor slip compared with further twinning inside the twinned grain. Therefore, more slip activity was observed in twinned regions in the case of coarse grain size material.

The twin volume fraction evolution measured in the fine grain size case is shown in Fig. 10. Simulations exhibit a close agreement with experimental evolution. Since very narrow twins form as bundles and look like a thick twin, it is hard to measure the volume fraction of matrix in between the twin lamellae with optical techniques. Hence, the difference between measurements and predictions can probably be attributed to the limitations of the experimental measurements.

Texture evolution in the case of polycrystalline materials was not predicted because the experimental texture evolution at low tensile strains was not significant.

7. DISCUSSION

The unique feature of this study is the introduction of a new hardening approach in a viscoplastic self-consistent constitutive model incorporating length scales associated with the microstructural evolution. The experimental stress–strain responses of single crystals with different crystallographic orientations and the polycrystalline materials with different grain sizes permit a critical check of the hardening approach. Our twinning reorientation scheme (PTR) captures the texture evolution accurately in the case of single crystal deformation in tension.

The self-consistent approach assumes every crystal as an inhomogeneous inclusion embedded in the homogeneous effective medium (HEM) which represents the polycrystal aggregate. An advantage of the viscoplastic self-consistent formulation is the consideration of local grain interactions. The strength of this interaction dictates how much plastic deformation can be accommodated by the crystal relative to its surroundings, and neither shape change nor stresses are enforced in the present method as in the full constraints or the relaxed constraints cases [10, 11].

The VPSC formulation circumvents the restrictions of the Taylor or Sachs approach. It is possible to tune the effective compliance tensor by changing the value of the parameter n in equation (8a) and thus the degree of matrix–crystal interaction. When n increases, the matrix becomes more compliant and the interaction between crystal and matrix

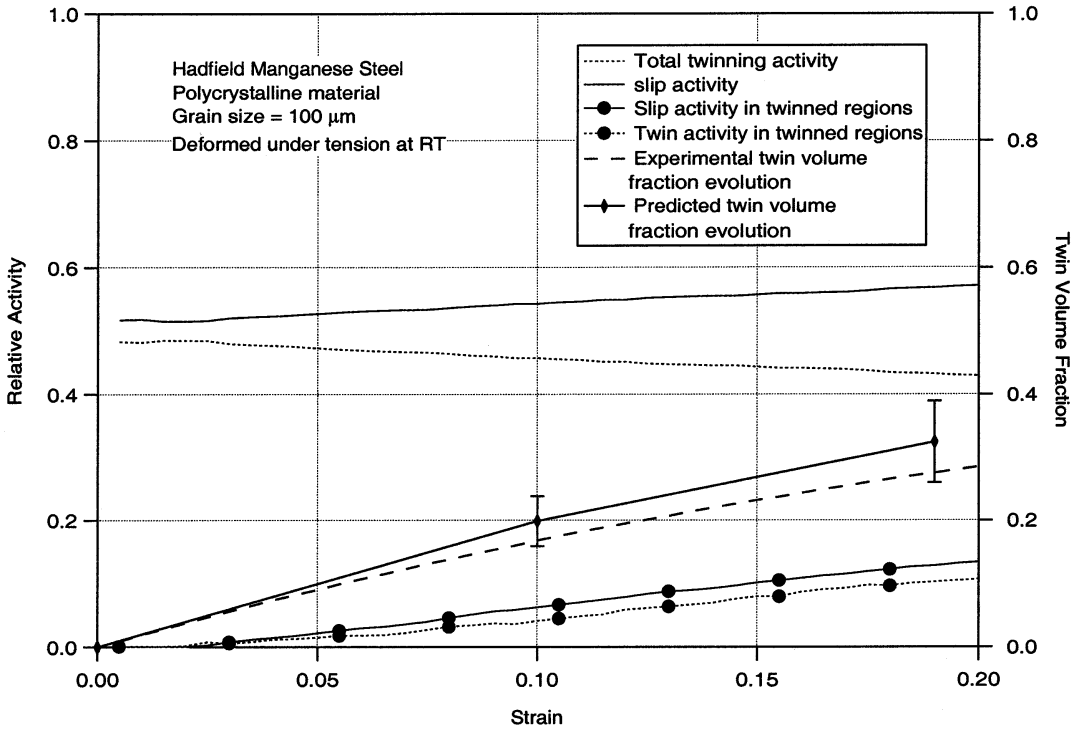

Fig. 10. The same as Fig. 9 for a grain size of 100 μm. The prediction of the twin volume fraction evolution fits the experimental ones well.

decreases. In the case of high anisotropy between the crystal and the matrix, such as in hexagonal materials, the interaction will play an important role on the overall plastic deformation. However, the anisotropy in f.c.c. materials is not as severe as in hexagonal materials. Therefore, n in equation (2) is chosen to be in the rate insensitive limit ($n = 20$).

In the self-consistent formulation, the stress–strain relation is linearized by the secant formulation. Another possible method in this linearization is the tangent formulation. Within the tangent framework soft grains deform more than average, while hard grains deform less. In the secant approach, every grain is strongly constrained by the surrounding matrix and deforms similarly [34]. Both approaches are approximations to reality but in the present study they predicted similar stress–strain responses without significant differences. This is because the current material is more isotropic as compared with hexagonal materials.

To incorporate twinning into crystal plasticity models without dealing with the abrupt increase in computation times as mentioned in Section 4, Van Houtte [35], using statistical considerations, proposed firstly a scheme that does not increase the number of orientations throughout the deformation. In his model, the probability of the reorientation of a whole grain by twinning is given by the twinning fraction increment Δg in the grain, and the probability of reorientation by slip is $(1 - \Delta g)$. All twinning systems are scanned and the grain is completely reoriented by twinning if the outcome of a random number generator falls in the interval 0–Δg. Tomé *et al.* [7] argued that in Van Houtte's model, a large number of initial orientations is required in order for the statistical criterion to be meaningful. Moreover, since reorientation is based on the increments of the twin volume fractions in a given time step (independent of previous deformation history), the twinned orientation may not be the most dominant one in that particular grain. To overcome these difficulties, Tomé *et al.* [7] proposed two alternative twinning reorientation schemes. The one that is implemented in this study is the "predominant twin reorientation (PTR)" scheme. A threshold twinning volume fraction criterion was used to reorient the crystals and the accumulated volume fraction of twins due to reorientation was maintained consistent with the real volume fraction associated with the twinning shears [7]. The PTR scheme also accounts for the deformation history that is an advantage over their other scheme, the volume fraction transfer (VFT) and therefore, it is utilized in the present study.

Kalidindi [8] and Staroselsky and Anand [6] utilized FEM to simulate slip and twinning. In Kalidindi's study [8], the volume fraction evolution for twinning was defined as a simple power law function of the ratio of applied stress to twinning deformation resistance. Staroselsky and Anand [6] used Van Houtte's statistical approach [35] for grain reorientation due to twinning. Before reorientation, twinning shear was accounted for as providing a directional shear strain. Their relation does not include the effect of the current volume fraction of twinned regions. In reality, twinning rate decreases with increasing twin volume fraction in the crystal as shown in Section 6. Consequently, the current twinning content should be taken into account when modeling the evolution of twinning volume.

The significance of the present model is the ease of incorporating twinning as a deformation mode. While previous VPSC modeling efforts have proposed zero strain hardening or utilized empirical hardening laws, in this work we present dislocation density and volume fraction of twins as explicit variables. For the strain-hardening model to hold for Hadfield steel simulations, dislocations should be activated both parallel and perpendicular to the twinning plane such that multiple slip could occur. The TEM images (Fig. 2) showing tangled dislocations confirm that multiple slip has occurred in these cases. The simulations for polycrystals predicted an average of four to five activated slip systems with a significant shear activity in most of the grains.

The hardening law in equation (21) is assumed to be valid for both the slip and twinning systems and no distinction is made between two deformation mechanisms at this point. The d_1 in equation (21) is a general parameter which mimics the distance between twin lamellae, however, no attempt is made in the model to account for directionality of the lamellae. This approach is completely reliable in the case of polycrystalline materials because optical microscopy observations indicated that only one twin system prevails in every grain. Moreover, the distance between two lamellae is nearly constant. In these observations, there are more twin systems activated near grain boundaries to satisfy compatibility. This can be viewed as a further constraint for dislocation motion at the grain boundaries, and supports our approach for differentiating between the strengths of two types of boundaries (twin and grain) with the constants K_0' and K_0''. In the case of single crystals, multiple twin systems are active especially in stage II and directionality of the lamellae may play a role in the hardening. Moreover, there should be a difference in hardening between slip systems whose Burgers vectors are perpendicular to the existing twin systems and those whose Burgers vectors are parallel to the existing twin systems due to dislocation reactions explained in Section 5. If there is more than one twin variant, then it is likely that a slip system will have a perpendicular twin boundary to interact strongly and equation (21) would be valid. In this work, however, we have considered the hardening of slip and twinning systems in an average sense without considering rela-

tive orientations of them with respect to boundaries. For a more precise approach, the geometrical factors K_0' and K_0'' can be defined as

$$K_0', K_0'' = f(\beta) \tag{23}$$

where β is the angle between the Burgers vector of a system and the boundary interface or other barriers.

In the present work, the twin–twin interaction is treated as similar to the slip–twin boundary (as a barrier) interaction considering that the twinning dislocations at the twin tip would interact with the existing twin boundary providing similar dislocation reactions as in Section 5. Although there are detailed studies of twin–twin interaction in f.c.c. intermetallics such as TiAl [36], to modify the hardening law, the nature of this interaction is not well understood for low stacking fault high strength steels. A detailed TEM study is needed to understand this interaction and to modify our hardening approach. However, as a first approximation to incorporate the twinning length scale into a crystal plasticity model, our hardening approach is proved to work well.

The focus of the paper is the room temperature deformation of single and polycrystal Hadfield steels to better understand the effect of slip and twinning together on the strain-hardening behavior. Therefore, the strain rate dependence of the strain-hardening coefficient is not included in this study since a previous study of one of the authors indicated that in the present material, two orders of magnitude change in the strain rate does not create a significant change in strain hardening of polycrystals at room temperature. Thus, the rate sensitivity n is taken to be in the rate insensitive limit at this temperature. To reveal the strain rate dependence of this material, strain jump tests should be conducted at higher temperatures. When the relative importance of the terms in the hardening law, equation (21), is concerned, the geometrical storage (first term) is the prevailing term in the formulation. The Voce term in this equation corresponding to the dynamic recovery does not play an important role in the present material at room temperature, as well. To better understand the role of dynamic recovery in the stress–strain behavior, high temperature experiments are needed to suppress twinning and trigger climb and cross-slip.

8. CONCLUSIONS

The present work supports the following conclusions:

1. The upward curvature in stress–strain curves was observed in single crystals favorably oriented for twinning and in coarse grain polycrystals. This "unusual" strain-hardening behavior was predicted accurately upon incorporating the length scale associated with the mfp between twin lamellae. TEM observations confirmed that the distance between microtwins is less than 1 μm and remains nearly constant during the deformation.
2. The simulations proved that once twinning spreads across the material, slip deformation between the twin lamellae and within the twinned regions governs the deformation behavior. Once the grains twin, subsequent twinning activity in those regions is limited. The average number of active systems (twin and slip) was nearly four throughout the deformation.
3. Experimental and simulated texture evolution in $[\bar{1}11]$ oriented single crystals agrees closely for the case of single crystals providing an additional check on the capabilities of the deformation modeling. In the case of coarse grain polycrystals, the initial texture was conducive to twinning deformation while for the fine grain polycrystals the initial texture was random favoring slip in addition to twinning. This explains the "linear" strain-hardening response in fine grain polycrystal instead of the "upward" curvature.
4. The results demonstrate that the strain-hardening behavior of coarse grain polycrystalline Hadfield steel is similar to that of $[\bar{1}11]$ single crystals. This result is consistent with the polycrystalline "coarse grain size" material having an initial texture favored towards the $[\bar{1}11]$ pole. The strain-hardening behavior at high strains exceeding 0.3 is limited by the damage evolution in [111] crystals, while in the [144] case the strain hardening extends to strains exceeding 0.6 providing a critical check on the model.

Acknowledgements—This work was supported by the National Science Foundation contract CMS 94-14525 and CMS 99-00090, Mechanics and Materials Program, Arlington, Virginia and a supplement from the NSF International Program. Y.I.C.'s work received support from The Russian Fund for Basic Research, Grant No. 02-95-00350. The facilities at Microanalysis of Materials, Materials Research Laboratory at The University of Illinois were used. This laboratory is funded by DOE-DMS grant DEFG02-96ER45439. The authors would like to thank the reviewer. The reviewer's comments led to refinement of hardening evolution [equation (21)].

REFERENCES

1. Adler, P. H., Olson, G. B. and Owen, W. S., *Metall. Trans.*, 1981, **12A**, 1725.
2. Dastur, Y. N. and Leslie, W. C., *Metall. Trans.*, 1981, **12A**, 749.
3. Karaman, I., Sehitoglu, H., Gall, K., Chumlyakov, Y. I. and Maier, H. J., *Acta metall. mater.*, 2000, **48**, 1345.
4. Asaro, R. J. and Needleman, A., *Acta metall.*, 1985, **33**, 923.
5. Lebensohn, R. A. and Tomé, C. N., *Acta metall. mater.*, 1993, **41**, 2611.

6. Staroselsky, A. and Anand, L., *J. Mech. Phys. Solids*, 1998, **46**, 671.
7. Tomé, C. N., Lebensohn, R. A. and Kocks, U. F., *Acta metall. mater.*, 1991, **39**, 2667.
8. Kalidindi, S. R., *J. Mech. Phys. Solids*, 1998, **46**, 267.
9. Kalidindi, S. R., *Int. J. Plasticity*, 1998, **14**, 1265.
10. Bishop, J. F. W. and Hill, R., *Phil. Mag.*, 1951, **42**, 414.
11. Honneff, H. and Mecking, H., in *Proc. Sixth Int. Conf. on Texture of Materials (ICOTOM-6)*, ed. S. Nagashima, 1981, p. 347.
12. Lebensohn, R. A. and Tomé, C. N., *Mater. Sci. Engng A*, 1994, **175**, 71.
13. El-Danaf, E., Kalidindi, S. R. and Doherty, R. D., *Metall. Mater. Trans.*, 1999, **30A**, 1223.
14. Acharya, A. and Beaudoin, A. J., *J. Mech. Phys. Solids*, submitted.
15. Mecking, H. and Kocks, U. F., *Acta metall.*, 1981, **29**, 1865.
16. Estrin, Y. and Mecking, H., *Acta metall.*, 1984, **32**, 57.
17. Kallend, J. S., Kocks, U. F., Rollett, A. D. and Wenk, R. H., *Mater. Sci. Engng*, 1991, **A132**, 1.
18. Hutchinson, J. W., *Proc. R. Soc.*, 1979, **A348**, 101.
19. Kocks, U. F., Tomé, C. N. and Wenk, R. H., *Texture and Anisotropy*. Cambridge University Press, Cambridge, 1998.
20. Lebensohn, R. A., Turner, P. A., Signorelli, J. W., Canova, G. R. and Tomé, C. N., *Modeling Simul. Mater. Sci. Engng*, 1998, **6**, 447.
21. Remy, L., *Metall. Trans. A*, 1981, **12A**, 387.
22. Mahajan, S., *Phil. Mag.*, 1971, **23**, 781.
23. Venables, J. A., in *Deformation Twinning*. Gordon & Breach, New York, 1964, p. 77.
24. Friedel, J., in *Dislocations*. Pergamon Press, Oxford, 1965, p. 182.
25. Kocks, U. F., Argon, A. S. and Ashby, M. F., *Prog. Mater. Sci.*, 1975, **19**, 1.
26. Kocks, U. F., in *Strength of Metals and Alloys*, ed. P. Haasen, V. Gerold and G. Kostorz. Pergamon Press, Oxford, 1979, p. 1661.
27. Remy, L., *Acta metall.*, 1978, **26**, 443.
28. Narita, N. and Takamura, J. I., in *Dislocations in Solids*. North-Holland, Amsterdam, 1992, p. 135.
29. Seeger, A., in *Structure and Mechanical Properties of Metals*. HMSO, London, 1963, p. 4.
30. Nabarro, F. R. N., Basinski, Z. S. and Holt, D. B., *Adv. Phys.*, 1964, **13**, 193.
31. Embury, D., Private communications, 1999.
32. Niewczas, M., Basinski, Z. S. and Embury, J. D., *Mater. Sci. Engng*, 1997, **A234–236**, 1030.
33. Mullner, P., *Mater. Sci. Engng A*, 1997, **A234–236**, 94.
34. Tomé, C. N., *Modeling Simul. Mater. Sci. Engng*, 1999, **7**, 1.
35. Van Houtte, P., *Acta metall.*, 1978, **26**, 591.
36. Sun, Y. Q., Hazzledine, P. M. and Christian, J. W., *Phil. Mag.*, 1993, **A68**, 471.